IFSCC 2025 full paper (IFSCC2025-1414)

The secret of cold Infrared(IRA) to human skin – mechanism of IRA-induced damage to dermal fibroblasts and keratinocytes and photoprotection method with functional liposomes

Jihui Jang[1], Chaewon So[2], Su Ji Kim[1], Heemuk Oh[1], Seoyoon Lee[1], Jihyun Lee[1], Sung Yun Hong[1], Hyeondo Lee[1], Chun Ho Park[1], and Hyejung Mok[2,*], and Jun Bae Lee[1,*]

[1]COSMAX R&I Center, Seongnam-si, Republic of Korea; [2]Department of Bioscience and Biotechnology, Konkuk University, Seoul, Republic of Korea

*Hyejung Mok, (Phone) +82-2-450-0448, hjmok@konkuk.ac.kr; *Jun Bae Lee, (Phone) +82-31-789-3192, (Fax) +82-31-8018-0221, jblee@cosmax.com

Abstract

This study investigated whether synergistic cellular damages could be induced by single near-infrared A (IRA) exposure combined with cold stress at 4°C (IRC) in human dermal fibroblasts and keratinocytes, based on cellular and mitochondrial reactive oxygen species (ROS) levels, apoptotic responses, cell migration, and photoaging. Sequential exposure to IRC significantly increased both cellular and mitochondrial ROS levels, inhibited cell migration, induced cellular apoptosis, and triggered senescence-associated β-galactosidase activity in fibroblasts. The severe biological damages in fibroblasts and keratinocytes by IRC could be effectively mitigated using the alpha-tocopherol-loaded liposomes (Toc/Lips; average size: 163.6 ± 18.7 nm; surface charge: –8.8 ± 1.8 mV). In addition, the highly stable Toc/Lips successfully protected tocopherol from IRA-induced photodegradation. Therefore, protecting skin cells using Toc/Lips may play a critical role in anti-aging and maintaining healthy skin tissue under daily environmental stresses.

Keywords: infrared-A ray, cold stress, alpha-tocopherol, liposome, fibroblast, keratinocyte

---

1. Introduction

IRA (700–1,400 nm) irradiation has received limited attention in the context of photoaging due to its relatively low energy compared to ultraviolet (UV) irradiation. In our previous study, acute IRA irradiation at a normal body temperature did not cause cellular damage in skin fibroblasts and keratinocytes [1].Only chronic and sustained IRA irradiation at normal temperatures was shown to cause severe photo-induced damage to skin cells by increasing ROS levels and enhancing apoptotic signaling. However, even though acute IRA exposure alone may be

insufficient to cause significant cellular damage, a single exposure to IRA combined with heat stress altered the expression of photoaging-related genes, such as matrix metalloproteinase-1 (MMP-1) [1]. A previous study found that natural-level solar radiation accompanied by heat (39°C) led to higher ROS levels and MMP-1 expression in human dermal fibroblasts compared to the same radiation at 37°C [2]. Additionally, both heat and cold stresses were reported to have synergistic damaging effects on skin cells. UV exposure following 3 hours of cold stress (4°C) caused substantial nuclear damage [3]. Given that average winter temperatures can fall below 4°C, cold-induced physical and chemical stress—termed cold stress—has become an unavoidable environmental factor in daily life. Thus, attention should be paid to the combined physical stresses that results from photo-induced damage at low temperatures. However, to our knowledge, synergistic skin damage caused by the combination of IRA and cold stress has not yet been investigated.

In this study, we investigated the synergistic cellular damage caused by single IRA exposure combined with cold stress at 4°C (IRC) in human dermal fibroblasts based on cellular and mitochondrial ROS levels. To evaluate the IRC-induced responses, including apoptosis, cell migration, and photoaging, fibroblasts were assessed using fluorescence-labeled Annexin V staining, wound healing assays, and senescence-associated β-galactosidase (SA-β-gal) activity assays. Furthermore, the effects of IRC on wound healing and cell morphology were compared between fibroblasts and keratinocytes after a single IRC exposure. For recovery of IRC-induced cellular damage, alpha-tocopherol (Toc)-incorporated liposomes (Toc/Lips) were fabricated and their physicochemical properties—including particle size, surface charge, morphology, tocopherol loading content, aqueous stability, and photostability—were characterized using dynamic light scattering (DLS), transmission electron microscopy (TEM), and high-performance liquid chromatography (HPLC). The protective effects of Toc/Lips against IRC-induced cellular damage were evaluated using mitosox assays, Annexin V staining, and wound healing assays

2. Materials and Methods

Materials

Fluorescein isothiocyanate (FITC)-labeled annexin V Apoptosis Detection Kit I was purchased from BD Biosciences. A MitosoxTM Red mitochondrial superoxide indicator, CellTracker™ red, and TRIzol® reagent were purchased from Thermo Fisher Science. Dulbecco's Modified Eagle's Medium (DMEM), penicillin/streptomycin, fetal bovine serum (FBS), and trypsin-EDTA were obtained from Gibco BRL. Toc, soybean L-α-lecithin (lecithin), DCFDA, trypan blue, 37% formaldehyde solution, mounting medium (Fluoroshield™ with 4',6-diamidino-2-phenylindole), a senescence cell histochemical staining kit, and phosphate buffered saline (PBS) were obtained from Sigma Aldrich. Human dermal fibroblasts and HaCaT keratinocytes were used.

ROS assay

The fibroblasts were irradiated one time with IRA for 4 h at 34°C at an irradiance of 42 mW/cm^2 and incubated at 4°C in a cold chamber for 3 h. After washing the cells with PBS solution, these were stained with DCFDA (20 μM) in serum-free DMEM without phenol red and incubated for 30 min at 37°C in the dark. After washing the cells with PBS solution, the cells were incubated for 20 min at 37°C in the dark. The mitochondrial ROS levels were determined using MitosoxTM Red mitochondrial superoxide indicator according to the manufacturer's protocol. After incubation, the cells were visualized using an inverted fluorescence microscopy.

Annexin V staining

After fibroblasts were exposed to IRC, cells were incubated for 24 h and washed with PBS solution and binding buffer (10 mM HEPES [pH 7.4], 140 mM NaCl, and 2.5 mM CaCl2). The

cells were then stained with FITC-labeled annexin V in binding buffer and incubated for 15 min at room temperature in the dark. After the cells were fixed with formaldehyde (3.7%) in PBS solution for 10 min and covered with mounting solution, these were visualized using an inverted fluorescence microscopy (Olympus).

Cell migration assay

Fibroblasts were seeded and incubated for 12 h, scratches were made with a 1 mL pipette tip. After the IRC were exposed to cells, cells were incubated for 24 h at 37°C and the scratches of each sample were observed by light microscopy.

SA-β-gal activity assay

After cells were exposed to IRC, and the SA-β-gal activity was assessed according to the manufacturer's protocol. Cells were visualized using a Cytation Hybrid Multi-Mode Reader (BioTek). The DAPI positive cells and SA-β-gal positive cells were analyzed with BioTek Gen5 software.

Preparation of Toc/Lip

The lecithin (15 mg) was mixed with Toc at different Toc/lecithin weight ratios (0, 0.2, 0.33, 0.5, and 1) in chloroform and evaporated in a rotary evaporator at 50°C. After evaporation, the thin film was hydrated with ammonium phosphate buffer (pH 7.4) and sonicated immediately for 5 min at 30% amplitude using a tip sonicator (Branson Digital Sonifier 450). The resulting solutions were purified by dialysis using a membrane (molecular weight cut-off of 25 kDa) in distilled water at room temperature. After purification, the average diameter of Toc/Lips was measured by DLS at 25°C using a Nano-S device (Malvern Instrument Ltd.). The surface charges of the Lips and Toc/Lips were measured using a Nano-ZS Zetasizer (Malvern Instruments, Ltd.). For the TEM analysis, the Toc/Lips were placed on a 300-mesh copper grid and air-dried. The grids were observed using a Bio-TEM instrument (Tecnai G2 Sprit Twin; FEI). The concentration of Toc within Lips was analyzed using RP-HPLC (Agilent Technologies) equipped with a diode-array detector on a Varian polar C18 reverse-phase column (4.60 × 250 mm, 0.45 μm; Varian). For the stability assay, Toc/Lips at a concentration of 0.2 mg/mL was incubated in DW and PBS solution at 4°C for predetermined time intervals and the particle size of the Toc/Lips was measured using DLS. After exposure to IRA for a predetermined time, the amount of Toc was measured using a UV spectrophotometer at a wavelength of 292 nm.

Protection of fibroblasts using Toc/Lip

Fibroblasts were treated with free Toc and Toc/Lip at a final Toc concentration of 40 μM. After incubation, the protective effect of Toc/Lips against IRC damage was evaluated using the wound healing assay, Mitosox assay for ROS, and Annexin V staining for apoptosis.

3. Results

Cellular responses to single IRC exposure

As shown in the following Figure 1A, skin cells were sequentially exposed to IRA irradiation at 34°C for 4 hours, followed by cold stress at 4°C for 3 hours. Cellular damage was evaluated by measuring ROS levels, Annexin V staining to detect apoptosis, cell migration assays, and SA-β-galactosidase (SA-β-gal) staining to assess cellular senescence. Toc/Lips were prepared via thin-film casting and hydration using lecithin dissolved in chloroform, in order to protect cells from severe damage induced by the dual physical stresses (Figure 1B).

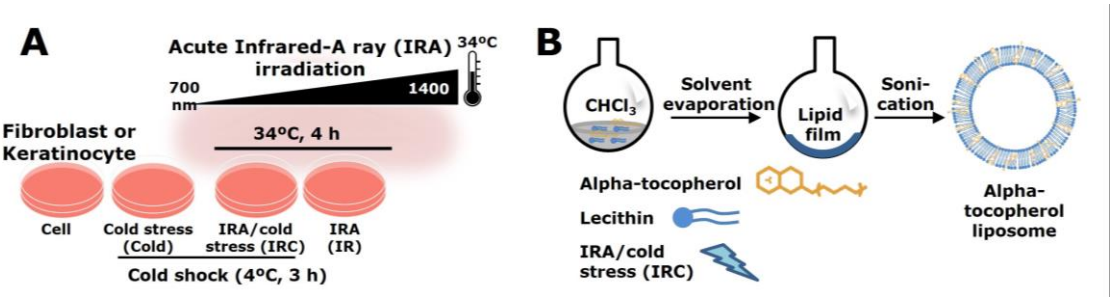

Figure 1. (A) Schemes for sequential exposure of IRC to cells. (B) Formulation of Toc/Lips via thin-film casting and hydration method

As shown in Figure 2A, IRC showed strong fluorescence signals in DCFDA assay and Mitosox assay, which indicates that IRC significantly increased cellular and mitochondrial ROS in fibroblasts compared to IRA or cold stress alone. IRC showed strong green fluorescent signals due to annexin V staining, which suggests that IRC might result in increased apoptosis in cells (Figure 2B). In addition, the extent of wound width was not reduced by IRC exposure probably due to decrased cell proliferation and migration (Figure 2C). IRC also induced cellular senescence, indicated by increased SA-β-gal activity (Figure 2D).

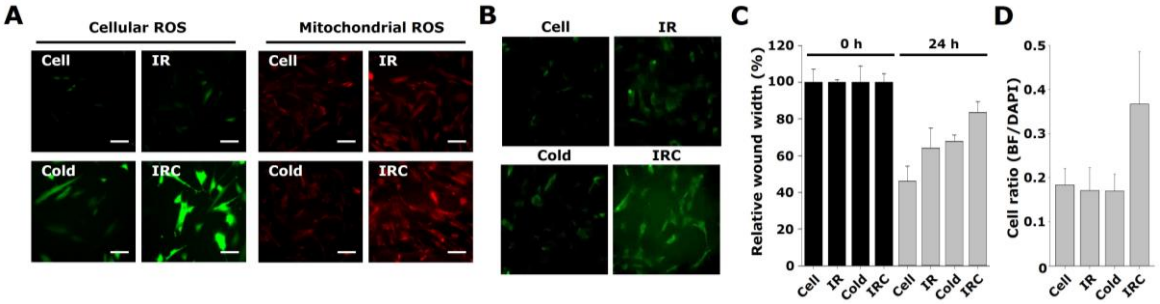

Figure 2. Cellular damages by IRC exposure. (A) ROS level by DCFDA assay and Mitosox assay. (B) Annexin V staining. (C) Cell migration assay. (D) SA-β-gal activity assay.

Formulation and characterization of Toc/Lip

Nanosized Toc/Lips were formulated with varying Toc/lecithin ratios (Figure 3A-C). The diameter of Lips, Toc/Lips at Toc/lecithin weight ratios of 0.2, 0.33, and 0.5 were 101.4 ± 12.4, 163.6 ± 18.7, 174.6 ± 14.7, and 249.9 ± 28.0 nm, respectively. As the Toc/lecithin weight ratio elevated, the diameter particle increased. The surface charge of Lips and Toc/Lips at a Toc/lecithin weight ratio of 0.2 was –11.3 ± 0.5 and –8.8 ± 1.8 mV. The amount of encapsulated Toc was quantitatively analyzed by HPLC (Figure 3D). The loading efficiency of Toc in Lips at Toc/lecithin weight ratios of 0.2 was 56.8 ± 10.6 %. A ratio of 0.2 was chosen for further experiments due to particle size and loading efficiency. Toc/Lips demonstrated good aqueous stability for 28 days. In addition, Toc was succssfully protected from IRA-induced degradation after liposome formulation, as shown in Figure 3F.

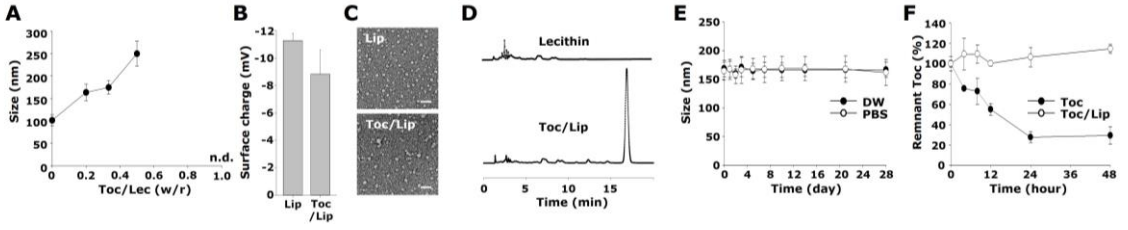

Figure 3. Characterization of Toc/Lip. (A) Particle sizes of Toc/Lip at different Toc/Lip weight ratios. (B) Surface charge, (C) TEM analysis, and (D) HPLC analysis of Toc/Lips at a Toc/lecithin weight ratio of 0.2. (E) Particle stability of Toc/Lip in DW and PBS for 28 days. (F) Photostability of Toc/Lip after IRA exposure for 48 h.

Protective effect by Toc/Lip from IRC-induced damages

Following Toc/Lip pretreatment, the cellular responses to single IRC exposure—including ROS levels, cell migration, and apoptosis—were evaluated to determine the protective effects of the formulation. As shown in Figure 4 A, pretreatment with Toc/Lips attenuated IRC-induced mitochondrial ROS level. In addition, the extent of annexin V staining in cells with Toc/Lips before IRC exposure was reduced in Figure 4B. The level of fluorescence intensity of annexin V staining was quantitatively analyzed in Figure 4C, which showed reduced apoptosis by Toc/Lips pretreatment in fibroblasts. Toc/Lip-pretreated cells showed enhanced wound closure compared with untreated cells after incubation for 36 and 48 h fibroblasts (Figure 4D). However, Toc and Toc/Lip exhibited similar anti-apoptotic activity and wound healing in Figure 4. IRC increased MMP-1 mRNA expression, which was reduced by Toc and Toc/Lips pretreatment. IL-6 mRNA expression decreased with IRC, while BAX expression was unaffected. The study suggests Toc can be released from Toc/Lips after uptake, providing protection against IRC damage. In addition, we believe that the developed material can maintain the photostability of the antioxidant against infrared light, thereby recovering skin cell damage caused by IRC.

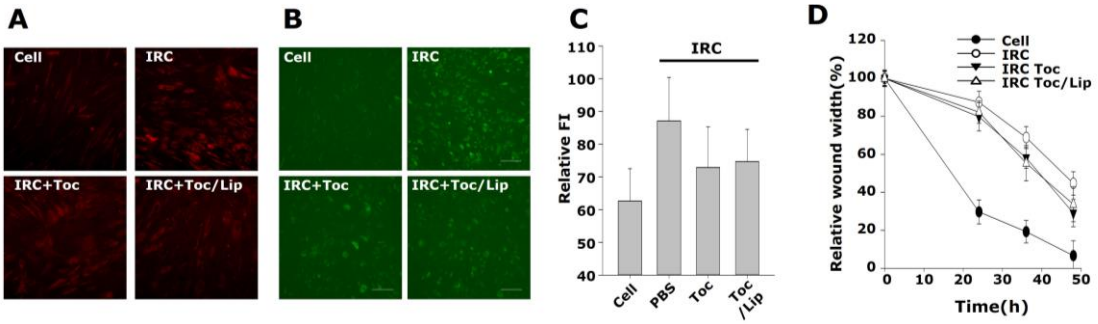

Figure 4. Protective effects of Toc/Lip against IRC-induced cellular damage. (A) Fluorescence microscopy images of the cells after Mitosox staining. (B) Fluorescence microscopy images of cells and (C) quantitative analysis of green fluorescence intensity (FI) in cells after Annexin V staining. (D) Quantitative analysis of wound width in the wound healing assay using ImageJ software.

4. Discussion

Previous research showed that while mild acute IRA caused minimal fibroblast damage, chronic exposure was harmful [1, 4]. Unlike UV and cold stress which induce apoptosis and bubbling cell death [3], the synergistic effects of IRA with other physical stresses are less understood due to IRA's lower energy. This study investigates the combined effects of IRA irradiation and cold stress (IRC) on skin cells, as daily life involves multiple stimuli. We examined if IRC increases damage in fibroblasts and keratinocytes by assessing ROS levels, apoptosis (annexin V staining), cell migration, and senescence (SA-β-gal assay) after sequential IRA (4h at 34°C) and cold (3h at 4°C) exposure, comparing it to single stimuli. As shown in the figures above, we observed that severe cellular damages including increased ROS and aopotosis could be elicited in skin cells due to single IRC treatment.

Photonic stimulation generates cellular and mitochondrial ROS, leading to apoptosis, reduced cell proliferation, and abnormal gene expression [5–7]. Accordingly, various antioxidants have traditionally been used to regenerate skin cells and mitigate skin aging. Nevertheless, conventional antioxidants such as Toc and vitamin C exhibit poor water solubility, low stability, and high sensitivity to environmental factors such as light, oxygen, and temperature, resulting in limited bioavailability [7,8]. To improve bioavailability and biological activity, nanomaterials have been introduced [9]. In our study, due to its biocompatibility, low cost, and environmental friendliness, lecithin has been widely used in liposome (Lip) formulations [10,11]. Previously, Toc-loaded liposomes (Toc/Lips) were prepared via the thin-film hydration method, showing improved membrane rigidity and antioxidant activity [12,13]. However, the protective effects of Toc/Lips against the synergistic skin damage caused by IRA irradiation combined with cold stress have not yet been examined. In this study, tocopherol-loaded liposomes (Toc/Lips) were formulated to protect cells from IRC damage, and their protective effects on ROS, cell migration, and apoptosis were evaluated. We confirmed that treatment with liposomes incorporating the antioxidant tocopherol showed a notable protective effects against IRC exposure on skin damage. Furthermore, we confirmed through Annexin V staining that Toc/Lips have an effect of reducing cell death caused by infrared/cold multiple stimulation. In addition, we confirmed that by encapsulating the antioxidant tocopherol inside liposomes, the liposome material has the advantage of maintaining high photostability of tocopherol. Figure 3F showed excellent photostability of Toc during storage and treatment in Toc/Lips, which might be crucial for skin protection in daily life. In addition, because nanosized emulsions have shown preferred tissue penetration and delivery of active Toc from the formulation) in previous studies, Toc/Lips below 200 nm could show improved skin permeability of Toc [14,15]. Accordingly, formulation of Toc using liposomes might be an advantageous approach to improve delivery efficiency of Toc into dermal fibroblasts and keratinocytes for the promising protection from IRC-mediated damages.

5. Conclusion

This study is the first to demonstrate that acute IRC severely damaged fibroblasts and keratinocytes and the damages could be mitigated by Tocopherol-loaded liposomes (Toc/Lip). Sequential IRC exposure significantly elevated cellular and mitochondrial ROS, leading to apoptosis, reduced cell migration, and cellular senescence in fibroblasts. Both fibroblasts and keratinocytes were susceptible to IRC. Toc/Lips (163.6 ± 18.7 nm, -8.8 ± 1.8 mV) effectively reduced IRC-induced mitochondrial ROS, apoptosis, and improved cell migration in fibroblasts. Furthermore, Toc/Lip exhibited high aqueous stability and protected Toc from IRA photodegradation. These findings highlight the importance of protecting skin from IRC for healthy aging and demonstrate the potential of Toc/Lips in preventing IRC-mediated skin damage in daily life.

Acknowledgements

This study was supported by a grant (NRF-2023R1A2C1005538) from the National Research Foundation, funded by the Ministry of Education, Science, and Technology and the Korea

Health Technology R&D Project through the Korea Health Industry Development Institute (KHIDI), funded by the Ministry of Health & Welfare, Republic of Korea (grant number : RS-2023-KH140863).

Conflict of interest statement

None.

References

1. Kim JY et al., “Protective effects of titanium dioxide-based emulsion after short-term and long-term infrared-A ray irradiation on skin cells” *Biotechnol Bioprocess Eng*, 26, 595–605 (2021)
2. Lan CC et al., “Solar-simulated radiation and heat treatment induced metalloproteinase-1 expression in cultured dermal fibroblasts via distinct pathways: implications on reduction of sun-associated aging” *J Dermatol Sci,* 72, 290–295 (2013)
3. Chen SJ et al., “UV irradiation/cold shock-mediated apoptosis is switched to bubbling cell death at low temperatures” *Oncotarget,* 6, 8007–8018 (2015)
4. Yang J et al., “Chronic infrared-A irradiation-induced photoaging of human dermal fibroblasts from different donors at physiological temperature” *Photodermatol Photoimmunol Photomed*, 38, 571–581 (2022)
5. Rezaei A et al., “Nanoencapsulation of hydrophobic and low-soluble food bioactive compounds within different nanocarriers” *Food Hydrocoll*, 88,146–162 (2019)
6. Maione-Silva L et al., “Ascorbic acid encapsulated into negatively charged liposomes exhibits increased skin permeation, retention and enhances collagen synthesis by fibroblasts” *Sci Rep*, 9, 522 (2019)
7. Camillo L et al., “Alpha-tocopherol protects human dermal fibroblasts by modulating nitric oxide release, mitochondrial function, redox status, and inflammation” *Skin Pharmacol Physiol,* 35, 1–12 (2022)
8. Gopi S et al., “Evaluation and clinical comparison studies on liposomal and non-liposomal ascorbic acid (vitamin C) and their enhanced bioavailability” *J Liposome Res,* 31, 356–364 (2021)
9. Na Y et al., “α-Tocopherol-loaded reactive oxygen species-scavenging ferrocene nanocapsules with high antioxidant efficacy for wound healing” *Int J Pharm*, 596, 120205 (2021)
10. Elnaggar YS et al., “Lecithin-based nanostructured gels for skin delivery: an update on state of art and recent applications” *J Control Release*, 180, 10–24 (2014)
11. van Hoogevest P et al., “The use of natural and synthetic phospholipids as pharmaceutical excipients” *Eur J Lipid Sci Technol*, 116, 1088–1107 (2014)
12. Xu T et al “Physicochemical properties, antioxidant activities and in vitro sustained release behaviour of co-encapsulated liposomes as vehicle for vitamin E and β-carotene” *J Sci Food Agric*, 102, 5759–5767 (2022)
13. Amiri S et al., “Vitamin E loaded nanoliposomes: effects of gammaoryzanol, polyethylene glycol and lauric acid on physicochemical properties” *Colloids Interface Sci Commun*, 26,1–6 (2018)
14. Ascenso A et al., “Development, characterization, and skin delivery studies of related ultradeformable vesicles: transfersomes, ethosomes, and transethosomes” *Int J Nanomedicine*, 10, 5837–5851 (2015)
15. Cichewicz A et al., “Cutaneous delivery of α-tocopherol and lipoic acid using microemulsions: influence of composition and charge” *J Pharm Pharmacol*, 65, 817–826 (2013)